Available online at www.sciencedirect.com

Polymer 46 (2005) 6102–6113

polymer

www.elsevier.com/locate/polymer

Analysis of the modulus of polyamide-6 silicate nanocomposites using moisture controlled variation of the matrix properties

D.P.N. Vlasveld[a,b], J. Groenewold[a,b], H.E.N. Bersee[c], E. Mendes[a,b], S.J. Picken[a,b,*]

[a]Polymer Materials and Engineering, Faculty of Applied Sciences, Delft University of Technology, Julianalaan 136, 2628 BL Delft, The Netherlands
[b]Dutch Polymer Institute, John F. Kennedylaan 2, P.O. Box 902, 5600 AX Eindhoven, The Netherlands
[c]Design and Production of Composite Structures, Faculty of Aerospace Engineering, Delft University of Technology, Kluyverweg 3, P.O. Box 5058, 2600 GB Delft, The Netherlands

Received 7 February 2005; accepted 12 April 2005
Available online 13 June 2005

Abstract

The stiffness of PA6 silicate nanocomposites has been measured for a number of silicate fractions and moisture levels. The matrix modulus was varied experimentally by moisture conditioning, resulting in three different moisture levels. The moduli have been analysed with a Halpin–Tsai composite model. This model was used to calculate the matrix modulus in the nanocomposites based on the crystallinity, the amount of surfactant and the moisture content. The measured modulus of the nanocomposites with different moisture content was used to calculate the effective aspect ratios of the reinforcing particles with the Halpin–Tsai model. The calculated aspect ratio for each nanocomposite is independent on the moisture concentration. This indicates the validity of this composite model to describe nanocomposites, despite the small particle size. The results suggest that changes on the molecular level due to the presence of the silicate layers only have a small influence on the modulus, because the modulus can be explained with a composite model. The reduced efficiency of reinforcement at increasing filler levels can be partially explained by the reduction of the matrix modulus due to surfactant and reduced crystallinity, and partially by the occurrence of small stacks of platelets.

Keywords: Modulus; Halpin–Tsai; Nanocomposite

1. Introduction

Polyamide-6 (PA6) nanocomposites containing exfoliated layered silicate particles can be produced by in situ polymerisation of ε-caprolactam [1–3] or by high shear mixing of the polymer in a twin-screw extruder [4–8]. Nanocomposites have been developed to improve the properties of polymers such as stiffness, flammability and barrier properties at a very low filler content. Compared to traditional filled polymers containing larger particles such as talc or glass fibres, nanocomposites have the additional advantage of a lower density and better surface smoothness and transparency. Nanocomposites can be transparent because the particle size is below the wavelength of visible light, so the particles do not cause scattering of light.

The most obvious enhancement in mechanical properties that layered silicates can provide is a large increase in modulus at very low filler concentrations. For example, 4% exfoliated layered silicate filler can give the same increase in modulus as 40% traditional mineral filler such as talc or 15% glass fibres [7]. The modulus increase is mainly in the long directions of the particles because of the high aspect ratio of the layered silicate particles. Compared to short fibre reinforcement the particle shape in layered silicate nanocomposites is more effective, because they can reinforce in two dimensions instead of one [9,10]. The stiffness and anisotropy of the particles also reduces thermal expansion and shrinkage upon crystallisation in the long direction of the platelets [11], although due to the anisotropy the expansion is larger in the thickness direction of the platelets [12,13].

Despite all the work done on nanocomposites, there is

---

* Corresponding author. Address: Polymer Materials and Engineering, Faculty of Applied Sciences, Delft University of Technology, Julianalaan 136, 2628 BL Delft, The Netherlands. Tel.: +31 15 278 6946; fax: +31 15 278 7415.
E-mail address: s.j.picken@tnw.tudelft.nl (S.J. Picken).

0032-3861/$ - see front matter © 2005 Elsevier Ltd. All rights reserved.
doi:10.1016/j.polymer.2005.04.087

still discussion about the reason of the large modulus increase by using such small amounts of filler. The nature of the mechanism is a subject of debate were various contrasting ideas seem to exist:

- The increased modulus could be contributed to the reduced mobility of a constrained polymer phase close to the silicate layers. The large surface area of the exfoliated platelets is considered to be responsible for this constrained polymer phase with a higher modulus [1,14,15].
- The strong ionic bond between the polymer and the silicate platelets is sometimes assumed to be the main reason for the enhanced modulus [16].
- The reinforcement mechanism in nanocomposites could be similar to traditional composites. In that case the modulus of the composite is dependent on the modulus of the matrix, the modulus of the filler and the shape and orientation of the filler particles. According to this view traditional composite theories can explain most of the properties of nanocomposites without assuming a change in the polymer properties [9,10].

In the first two theories the inherent modulus of the silicate particles is considered to be of minor importance, or even completely ignored. As has been shown by Van Es et al. and Fornes et al. [9,10] the presence of very stiff, high aspect ratio particles is expected to give a large increase in modulus and should not be ignored, as is sometimes done [14]. It is unlikely that the type of bond is very important for the modulus, because the bonding strength is not important for the modulus, although it is important for the strength of the composite. It has been reported that it is possible to make nanocomposites with layered silicates without any surfactant, which can give similar moduli [17], despite the lack of modification on the silicate filler.

By analysing the results of PA6 nanocomposites with different moisture content and describing this with a mechanical model we can add some valuable input to the discussion on the nature of the modulus of nanocomposites.

In this paper the influence of the silicate content and moisture content on the modulus of PA6 nanocomposites is described. The results obtained for the various moisture contents in the nanocomposites provide a good basis to test the validity of the Halpin–Tsai composite theory for nanocomposites. The experimental results are used to estimate the average platelet aspect ratio using the Halpin–Tsai composite model. The results of the model can show if nanocomposites behave like conventional composites or that the modulus of the matrix is changed by the presence of the nanoparticles, as is often suggested [1,14–16]. Composite models such as the series model, parallel model and Halpin–Tsai model assume that the matrix phase and the reinforcing phase do not change the properties of the other phase, so it is interesting to see to which extend this traditional composite model can predict the properties of nanocomposites. By changing the moisture content the modulus of the matrix can be varied over a wide range while the composition and morphology of the nanocomposites remains constant. The influence of the silicate on the crystallinity is measured with DSC and the orientation of the reinforcing platelets and the PA6 crystals is measured with WAXS. These parameters are used in the Halpin–Tsai model to estimate the matrix modulus in the nanocomposites and the effective aspect ratio of the silicate platelets. The calculated effective aspect ratios of the nanoparticles in nanocomposites with a wide variety of matrix moduli are compared to determine if the mechanism of modulus enhancement in layered silicate nanocomposites is similar to that of conventional (micro) composites.

2. Experimental

2.1. Materials

The polymer used to produce melt-blended nanocomposites is an injection-moulding grade of polyamide-6, Akulon K122D from DSM, The Netherlands.

An organically modified layered silicate based on natural montmorillonite clay, Cloisite™ 30 B from Southern Clay Products (USA), was used as nanoparticles. The manufacturer has added an organic surfactant (methyl-bis-2-hydroxyethyl tallow quaternary ammonium) on the silicate platelets to enhance the exfoliation by improving the interaction with the polymer. The amount of organic surfactant, approximately 32 wt%, is determined using thermo-gravimetric analysis (TGA).

Five different concentrations of Cloisite 30 B in polyamide-6 were used; all concentrations were conditioned to reach three different moisture levels.

2.2. Sample preparation

2.2.1. Extrusion

The nanocomposites were prepared by mixing Cloisite 30 B in PA6 in a Werner and Pfleiderer ZDS-K28 co-rotating twin-screw extruder. The modified layered silicate powder was mixed with the polymer granules and fed into the extruder at a constant rate via a Plasticolor 2500 feeding unit. The extruder was operated at a screw speed of 200 rpm and a feeding rate of approximately 3 kg/h, which resulted in an average residence time of 3 min in the extruder.

Temperature in the feeding zone was 150 °C, all the other zones where heated to 230 °C. Cooling was applied to keep the temperature constant since the high shear forces in the melt can produce too much heat. First a 10.6 wt% (based on the inorganic content of the filler) master batch was made. Other concentrations were made by diluting the master batch with unfilled K122D in a second extrusion step.

2.2.2. Injection moulding

Dumbbell shaped samples according to ISO 527 standard were injection moulded on an Arburg Allrounder 221-55-250 injection-moulding machine. The feeding zone was heated to 150 °C, the melting and mixing zones heated to 240 °C and the nozzle was kept at 260 °C. The mould was heated to a temperature of 90 °C to reduce the cooling speed and ensure a more homogeneous crystallisation.

2.2.3. Moisture conditioning

Dry as moulded samples were dried in a vacuum oven at 80 °C for at least 48 h before testing. The moisture conditioning was performed at 70 °C to increase the speed of moisture transport, which is necessary because of the barrier properties of nanocomposites. The sample weight was measured after drying and conditioning on a Mettler AE-240 to calculate the moisture level. The moisture content was calculated based on the amount of polyamide-6, so the silicate and surfactant weight were not included.

Samples with 3% water in the PA6 phase were prepared by conditioning in a Heraeus climate chamber at 70 °C and 65% relative humidity and samples with 6% water in the PA6 phase were prepared by conditioning at 70 °C and 92% relative humidity.

2.3. Testing

2.3.1. Measurement of silicate content

Thermogravimetric analysis (TGA) measurements were done to determine the exact silicate content in the tested samples after processing. A Perkin–Elmer TGA-7 thermal gravimetric analyzer was used to determine the weight fraction of silicate by heating a sample in air at 800 °C for 1 h.

2.3.2. Measurement of the crystallinity

The level of crystallinity of the samples and the ratio of the two crystal phases, α and γ, was determined with differential scanning calorimetry on a Perkin–Elmer DSC-7. DSC samples of approximately 5 mg were cut from the centre of the tensile test bar. The DSC measurements were performed at a heating rate of 10 °C/min between 25 and 270 °C. The crystallinity was calculated using a heat of fusion of 213 J/g for the gamma crystals, and 243 J/g for the alpha crystals [13].

2.3.3. Measurement of the glass transition temperature

The glass transition temperatures (T_g) of the samples were determined with dynamic mechanical analysis. Samples of 0.5 mm thin were cut from the injection moulded test bars and tested in three point bending in a Perkin–Elmer DMA 7e at a temperature range from −130 to 210 °C. The temperature at the highest point of the largest peak in the loss modulus spectrum was used to represent the T_g. The tests were done for unfilled PA6 and 6.7% silicate filled samples at moisture contents of 0, 3 and 6 wt% water in the PA6 phase.

2.3.4. Measurement of the average crystal and silicate platelet orientation

Wide angle X-ray scattering (WAXS) has been performed on a Bruker D8 Discover diffractometer with a 2D (1024 × 1024) detector using a 10 cm sample to detector distance and incident Cu radiation of 1.54 Å was used. An incident beam cross-section of 0.5 mm was used. A 0.5 mm thin cross section was cut through the thickness and the width of the moulded sample tensile test bar and X-ray measurements were taken at different positions starting from the edge and each next measurement 0.5 mm further inside the moulded sample.

2.3.5. Measurement of the modulus

The samples were tested on a Zwick 1445 tensile tester with a 10 kN force cell. For the modulus measurement Zwick clip-on extensometers were used. The test speed was 5 mm/min and the temperature was 23 °C.

3. Composite theory

The modulus of PA6 is strongly influenced by moisture absorption, therefore different moisture levels can be used to change the modulus of the matrix material without changing the microstructure of the nanocomposite.

The amount of water that can be absorbed by PA6 nanocomposites is not reduced compared to unfilled PA6, however, the rate of absorption is reduced due to the lower diffusion coefficient [18,19]. The water is absorbed in the amorphous part of PA6 [20], so in the model it is assumed that the absorbed water does not influence the mechanical properties of the crystalline phase. However, the amorphous phase shows a dramatic change in modulus because the absorbed moisture causes a decrease of the glass transition temperature to below room temperature. The matrix moduli are measured on the conditioned unfilled polymer, and they are subsequently compensated for the differences in crystallinity and the presence of surfactant with the Halpin–Tsai model. The aspect ratio of the reinforcing particles in each nanocomposite is calculated using the Halpin–Tsai model with the measured modulus of the nanocomposites and the different matrix moduli for the three different moisture contents as input.

3.1. The Halpin–Tsai model

In this article the semi-empirical Halpin–Tsai model [21, 22] is used, because it is a relatively simple but accurate model that takes into account the shape and the aspect ratio of the reinforcing particles. Polydispersity of the reinforcing particles in such a semi-empirical model will lead to an average particle size as a result. The Halpin–Tsai model was originally developed to describe the properties of semi-crystalline polymers [13,21], which are in essence also nanocomposites, and can also be used for composites reinforced with fibre and platelet shaped particles. Van Es [9,13,21] has derived a set of shape factors for platelet-reinforced composites by comparing results from the Halpin–Tsai equations to results from more fundamental approaches i.e. the Eshelby theory, the Mori–Tanaka theory and 3D finite element modelling [13,21].

Eq. (1) shows the traditional way [21] of writing the Halpin–Tsai equations:

$$\frac{E_\mathrm{c}}{E_\mathrm{m}} = \frac{1+\varsigma\eta\phi_\mathrm{f}}{1-\eta\phi_\mathrm{f}} \quad \text{in which } \eta = \frac{(E_\mathrm{f}/E_\mathrm{m})-1}{(E_\mathrm{f}/E_\mathrm{m})+\varsigma} \tag{1}$$

E_c, composite Young's modulus; E_f, filler modulus; E_m, matrix modulus; ζ, shape factor, depending on the geometry, orientation and aspect ratio of the particles; ϕ_f, volume fraction filler.

The shape factors for the tensile moduli of platelet reinforced composites are [9]:

E_{11} or E_{22} $\quad \zeta = 2/3\ (w/t)$

(in the radial direction of the platelets)

E_{33} $\quad \zeta = 2$ (perpendicular to the platelets)

(w/t) = width of platelet/thickness of platelet = aspect ratio.

When Eq. (1) is rewritten in one equation as is shown in Eq. (2), the nature of the Halpin–Tsai model becomes clearer.

$$E_\mathrm{c} = E_\mathrm{m}\frac{E_\mathrm{f}(1+\varsigma\phi_\mathrm{f})+E_\mathrm{m}(\varsigma-\varsigma\phi_\mathrm{f})}{E_\mathrm{f}(1-\phi_\mathrm{f})+E_\mathrm{m}(\varsigma+\phi_\mathrm{f})} \quad \text{(Halpin–Tsai)} \tag{2}$$

When the aspect ratios are much smaller then the ratio of filler and matrix modulus ($\zeta \ll E_\mathrm{f}/E_\mathrm{m}$) the Halpin–Tsai model gives results close to a series model:

$$E_\mathrm{c} \approx \frac{E_\mathrm{m}E_\mathrm{f}}{E_\mathrm{f}(1-\phi_\mathrm{f})+E_\mathrm{m}(\phi_\mathrm{f})} = \left(\frac{1-\phi_\mathrm{f}}{E_\mathrm{m}}+\frac{\phi_\mathrm{f}}{E_\mathrm{f}}\right)^{-1} \quad \text{(Series model)} \tag{3}$$

When the aspect ratios are much larger then the ratio of filler and matrix modulus ($\zeta \gg E_\mathrm{f}/E_\mathrm{m}$) the Halpin–Tsai model gives results close to a parallel model:

$$E_\mathrm{c} \approx E_\mathrm{m}\frac{E_\mathrm{f}\varsigma\phi_\mathrm{f}+E_\mathrm{m}\varsigma(1-\phi_\mathrm{f})}{E_\mathrm{m}\varsigma} = E_\mathrm{f}\phi_\mathrm{f}+E_\mathrm{m}(1-\phi_\mathrm{f}) \quad \text{(Parallel model)} \tag{4}$$

For nanocomposites the series model underestimates the modulus, because the volume fraction of filler is very low, resulting in domination of the first term in Eq. (3) and thus in values close to the matrix modulus. However, the parallel model overestimates the composite modulus at low matrix moduli, since it assumes a continuous reinforcing phase. The Halpin–Tsai model (Eq. (2)) leads to results that are in between these two extremes when the aspect ratio is of the same order of magnitude as the ratio of moduli ($\zeta \approx E_\mathrm{f}/E_\mathrm{m}$). The aspect ratio of the particles has a strong influence on the results and, therefore, determines how close the results are to either the series or parallel model. The calculated effect of the aspect ratio on the relative modulus ($E_\mathrm{composite}/E_\mathrm{matrix}$) in the Halpin–Tsai model for a platelet filled composite ($E_\mathrm{matrix} = 3.1$ GPa, $E_\mathrm{filler} = 172$ GPa, $\phi_\mathrm{f} = 0.05$) is shown in Fig. 1, which shows that the particles are hardly effective below $w/t = 10$, and only when w/t is above 1000 the maximum effect is reached.

This means that for typical platelet sizes in nanocomposites, the influence of the aspect ratio and, therefore, also of the exfoliation, on the modulus is very important. Platelet aspect ratios for layered silicate nanocomposites are around 100–200, consequently when exfoliation is not optimal the resulting reduction in aspect ratio has a large effect on the modulus. The Halpin–Tsai model can, besides calculation of the composite modulus, also be used to calculate the aspect ratio of the reinforcing particles when the modulus of the composite, matrix and filler are known. The Halpin–Tsai model can only give an effective aspect ratio, because the particles can have different shapes, sizes and thickness. The effective aspect ratio represents the best fit with the measured modulus data and can be considered a useful parameter to compare different nanocomposite compositions, as well as providing a reasonable estimate of the average aspect ratio.

In this paper the Halpin–Tsai model for a platelet reinforced composite is used twice:

1. To calculate the modulus of the matrix, based on the crystallinity and the amount of surfactant (Section 3.2).
2. To calculate the effective aspect ratio of the reinforcing particles in the nanocomposite (Section 3.3).

In the second model the results of the first model, i.e. the matrix moduli for each composition and moisture content, are used as input.

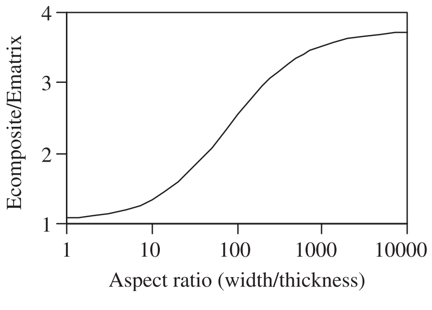

Fig. 1. Relative modulus as a function of aspect ratio for platelets (5 vol%, $E_\mathrm{m} = 3.1$ GPa, $E_\mathrm{f} = 172$ GPa).

3.2. Calculation of the matrix modulus using the Halpin–Tsai model

As mentioned before, the Halpin–Tsai model for nanocomposites assumes that the filler does not influence the properties of the matrix. However, the addition of the layered silicate filler can influence the modulus of the matrix because of its influence on the crystallinity and the presence of the surfactant.

- Surfactant: by adding the modified layered silicate also approximately half of its weight in anionic surfactant is added. The volume fraction is even larger than the weight fraction due to the lower density of the surfactant, and, therefore, the surfactant fraction should not be neglected.
- Crystallinity: it is known that the addition of layered silicates can influence the crystallinity. The crystallinity has a strong influence on the modulus of the matrix, especially above T_g, where the modulus mainly depends on the crystalline phase.

These two factors are accounted for by using a different matrix modulus for each silicate concentration in the Halpin–Tsai model to calculate the aspect ratios in the nanocomposites. The matrix moduli are calculated with the Halpin–Tsai equations because the semi-crystalline polymer can be considered to be a composite with an amorphous polymer matrix reinforced with crystalline polymer platelets (lamellae).

Although a nanocomposite based on a semi-crystalline polymer is a very complex system containing many different phases that can influence each other, we have assumed a simplified composition to be able to estimate the properties with a relatively simple composite model. The four phases of the simplified composition that is assumed in our model is shown in Fig. 2. It consists of a crystalline PA6 phase, an amorphous PA6 phase, a surfactant phase and an inorganic silicate phase.

The nanocomposite matrix consists of the crystalline PA6 phase, the amorphous PA6 phase and the surfactant phase. The modulus of the nanocomposite matrix is calculated with the Halpin–Tsai model that considers an amorphous matrix reinforced with crystalline platelets. The amorphous part of the matrix consists of amorphous PA6 and surfactant, and it is assumed in this model that the surfactant has no stiffness ($E_{\text{surfactant}}=0$). Therefore, the modulus of the amorphous matrix is calculated with Eq. (5):

$$E_{\text{amorphous matrix}} = E_{\text{amorphous PA6}}(1-\phi_{\text{surfactant}}) \qquad (5)$$

$\phi_{\text{surfactant}}$ = volume fraction surfactant in amorphous matrix

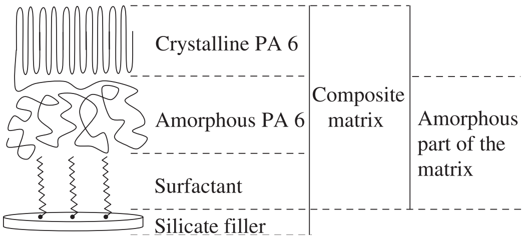

Fig. 2. Simplified composition of the nanocomposite for the Halpin–Tsai model.

The result is that the modulus of the amorphous phase in the model is slightly reduced when the modified silicate is added. The input for the Halpin–Tsai model to calculate the matrix modulus is the amorphous PA6 modulus, the modulus of the crystalline phase, the volume fraction of the crystalline phase, and the aspect ratio of the crystalline lamellae:

- Modulus of amorphous PA6

The value used for the modulus of dry amorphous PA6 at room temperature is 2.2 GPa, which is calculated from literature results for moduli at different amounts of crystallinity [23]. For moisture-conditioned samples with 3 and 6% water the value for the amorphous modulus is calculated with the Halpin–Tsai model from the measured sample modulus and the calculated crystalline modulus.

- Crystalline volume fraction

The heat required for melting in the tested samples was measured with DSC and with the use of the mass fractions of silicate and surfactant and the heat of crystallisation of the crystals ($\Delta H_{\text{alpha crystal}}=243$ J/g, $\Delta H_{\text{gamma crystal}}=213$ J/g [9]) the crystalline volume fraction of the matrix has been calculated.

- Aspect ratio of the crystalline lamellae

For the aspect ratio of the crystalline lamellae a constant value of 1000 is chosen in our model. Consequently, at these high values the modulus is almost independent on the exact aspect ratio, which was shown in Fig. 2. It is believed such a high aspect ratio is a reasonable assumption because the lamellae are very thin, around 5 nm [20], but relatively wide (several micro meter). It will be explained in the discussion (Section 4.3) why the exact value is not important in our calculations.

- Modulus crystalline phase

The crystalline phase can consist of several different crystalline structures, such as the α and γ-crystal structures. In this composite model it is assumed that the modulus of all crystal structures is identical. In our model the modulus in the long direction of the crystalline platelet is used, which is perpendicular to the chain axis. In the literature not much data is available for this direction of the crystal, and the values that have been reported are rather diverse [24]. However, it is possible to calculate the effective crystalline modulus with the Halpin–Tsai model by using the measured modulus of the dry polyamide-6 samples and the amorphous modulus. The calculated value for the crystalline modulus is used for all other samples to calculate how the matrix modulus changes with the crystallinity.

The result of this approach is a different matrix modulus for each nanocomposite sample, which depends on the crystallinity, the amount of surfactant and the moisture content.

3.3. Calculation of the effective platelet aspect ratio

The calculated matrix moduli for each sample can be used in the Halpin–Tsai model to calculate the effective aspect ratio of the silicate particles in the samples. Besides the matrix modulus, the input for this model is the modulus of each nanocomposite sample as measured on the injection moulded samples, the volume fraction silicate platelets as calculated from TGA measurements and the silicate modulus. The degree of alignment of the platelets is investigated using WAXS. In this model the modulus of the silicate platelets is assumed to be 172 GPa, equal to the modulus of a perfect mica crystal [25], which is comparable in structure to the layered silicates in our samples. The volume fractions are calculated from the mass fractions by using the following densities: ρ surfactant $=0.93$ g/cm^3 [26], ρ amorphous PA6 $=1.08$ g/cm^3, ρ α-crystalline PA6 $=1.24$ g/cm^3, ρ γ-crystalline PA6 $=1.18$ g/cm^3 [20,27], ρ silicate $=2.8$ g/cm^3 (equal to the density of mica [28]).

The modelled aspect ratios for each silicate concentration and moisture content are plotted versus silicate content to see if they show the same trend for each matrix modulus. If the aspect ratios are independent of the matrix modulus, this provides support to the idea that the stiffness of nanocomposites is based on the same mechanism as traditional composites.

Many simplifications in the composition for the model have been made and of several parameters the exact values are uncertain or subject of debate. However, small variations in the assumed values do not have a significant influence on the results and do not change the overall conclusions. The T_g's are similar for unfilled PA6 and nanocomposites.

4. Results and discussion

4.1. Silicate content, matrix crystallinity and T_g

The silicate levels as measured with TGA and the results are shown in the first row in Table 1. These values were used to calculate the silicate volume fraction, which is shown in the second row of Table 1.

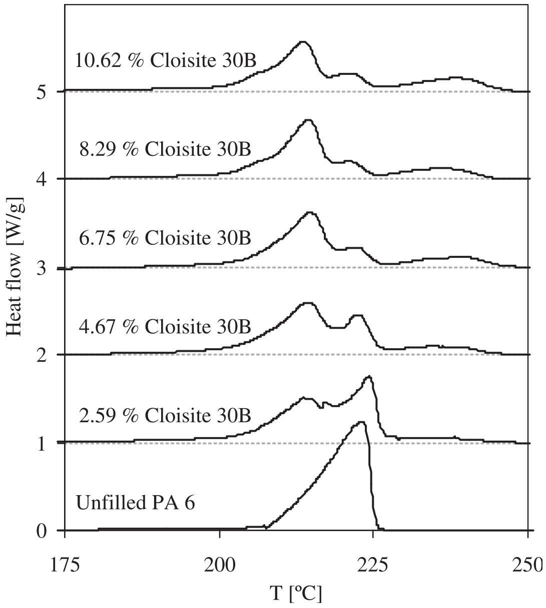

Fig. 3. DSC melting curves first heating (curves are shifted up for clarity).

The melting curves of the first heating sequence in the DSC measurements are shown in Fig. 3 (curves are shifted up for clarity).

The peak surface for the γ-crystal phase around 213 °C increases while the peak surface for the α-crystal phase around 220 °C decreases upon addition of silicate. In addition a new peak around 240 °C appears, which is also associated with the γ-crystal phase, as was shown by IR results [13]. The higher melting point could be the result of a higher lamellar thickness or of a stabilisation of the crystals due to interactions with the silicate. The ratio of α to γ-phase is estimated based on the relative peak areas in the DSC curves (fourth row in Table 1). The exact value of the ratio does not influence the results much because the heat of melting is very similar. The results for the heat of melting in combination with the α to γ-crystal ratio are used to calculate the percentage crystallinity in the samples. The crystallinity (wt%) based on the total PA6 content is shown in the third row of Table 1. In the last two rows of Table 1 the volume fractions of surfactant and crystalline PA6 are shown with respect to the total matrix of the nanocomposite, so this includes the PA6 and surfactant, but not the silicate filler. It can be seen that the volume fraction of crystalline matrix decreases slightly with increasing silicate content,

Table 1
Results TGA and DSC with calculated volume fractions

Properties nanocomposites	PA6	2.6%	4.7%	6.8%	8.3%	10.6%
wt% silicate (TGA)	0	2.6	4.7	6.8	8.3	10.6
vol% silicate	0	1.1	1.9	2.8	3.5	4.5
Fraction alpha crystalline	0.9	0.5	0.25	0.2	0.15	0.15
wt% crystalline PA6 in PA6	36.3	36.5	36.0	35.0	33.8	33.2
vol% surfactant in matrix	0	1.5	2.8	4.1	5.1	6.7
vol% crystalline PA6 in matrix	33.4	33.4	32.8	31.4	30.1	29.1

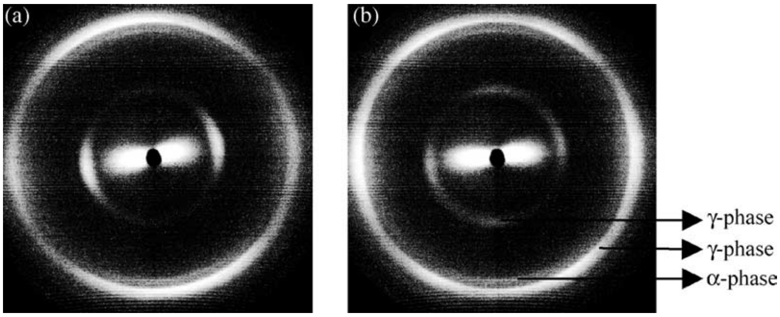

Fig. 4. WAXS spectrum 4.7% cloisite 30B nanocomposite. (a) 1 mm from the edge, (b) 0.5 mm from the edge.

while the surfactant fraction increases. Both changes probably lead to a reduction in matrix modulus at increasing filler levels, because the amorphous modulus is lower than the crystalline modulus and the surfactant does not add stiffness to the polymer. These results are used in the Halpin–Tsai model for the calculation of the matrix modulus.

The glass transition temperatures determined from the loss peak of the DMA measurements are 65 °C for the dry polymer, 25 °C for the polymer with 3 wt% water and 0 °C for the polymer with 6% water.

4.2. Silicate platelet and crystalline orientation

Two typical 2D WAXS scattering spectra are displayed in Fig. 4. The intensity rings at high scattering angles relate to the crystalline PA6 phases. The brightest high angle ring is associated with the γ-phase and the fainter ring inside is associated with the α-phase, the ring at intermediate angles is also associated with the γ-phase [20].

It can be seen from the figure that for a given spatial position inside the moulded bar, partial orientation of crystallites is observed. Such partial crystal orientation is strongly coupled to the observed oriented central scattering pattern present at smaller angles. This central scattering is the high angle limit of the form factor of the silicate platelets that are oriented with the flow direction. Although there is partial coupling between the orientation of platelets and the crystallites, the full dependence of crystal orientation inside the macroscopic sample seems a complex issue. This can be seen from the comparison of Fig. 4(a) and for Fig. 4(b) taken at two neighbouring positions inside the sample: in Fig. 4(a) the crystallite scattering seems to fully align with the platelets (central scattering) while in Fig. 4(b), it seems that a biaxial orientation is present. Also, as it can be seen from the same figures, α and γ-phases seem to orient differently along the sample. Furthermore, the average crystal orientation along the macroscopic sample may be evaluated by considering data grouped along the 2θ direction for different positions within the sample as displayed in Fig. 5. It can be seen from data on the γ-phase that even from this phase which is strongly induced by the silicate surface, crystal orientation at different positions along the sample seem to be uncorrelated. It is, therefore, reasonable to assume an average random orientation of crystallites along the macroscopic sample.

The absence of an inter-particle maximum in the scattering spectra indicates a very high degree of exfoliation. Consequently, the quantification of a degree of alignment by considering a silicate peak is impossible using WAXS. One way to relatively estimate the variation of the degree of orientation of the platelets along the sample

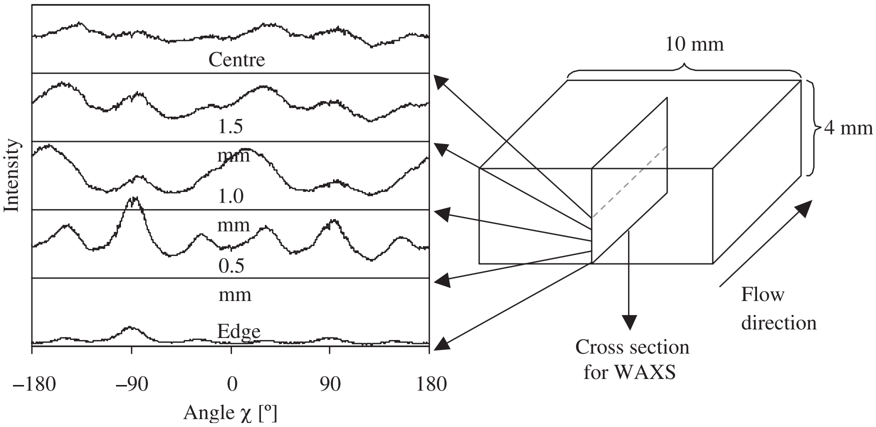

Fig. 5. WAXS peaks for the γ-crystalline phase (peak around 21°) at various depths within the injection moulded sample (4.7 wt% cloisite 30B). Curves are shifted up for clarity; the horizontal line below each curve is the baseline. On the right the orientation of the cross section within the injection moulded test bar is shown, and at which points the measurements are done.

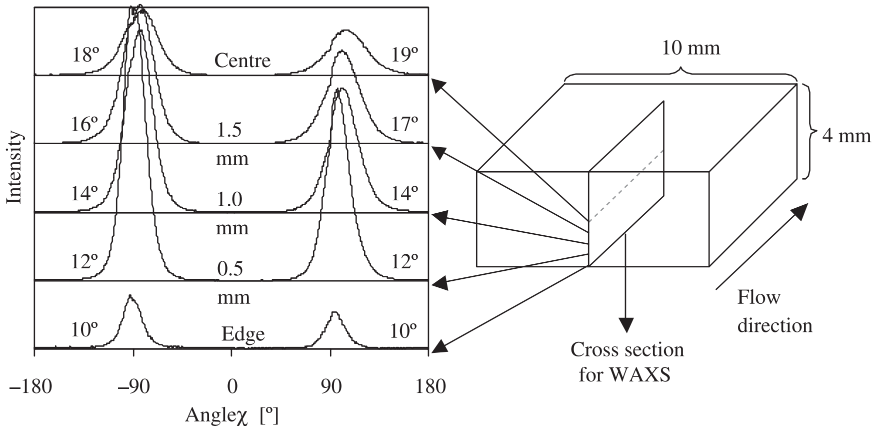

Fig. 6. WAXS results for the shoulder of the central scattering around the beam stop, which is used to estimate the orientation of the layered silicate at various depths. (4.7 wt% cloisite 30B). Curves are shifted up for clarity; the horizontal line below each curve is the baseline. The angles next to the peaks are the width at half the height. On the right the orientation of the cross section within the injection moulded test bar is shown, and at which points the measurements are done.

is to consider integrating the data associated with the shoulder of the central scattering around the beam stop along the 2θ direction. It was decided to arbitrarily integrate data in 2θ between 1.1° (next to the beam stop) and 7.9°. The resulting intensity as a function of the azimuthal angle χ is displayed in Fig. 6.

In order to estimate the orientation, the 'shoulder width' at half of the peak height was then calculated for each position along the sample and the values are displayed in Fig. 6. They vary between 10 and 19°, suggesting a very high degree of orientation along the sample. Performing the same set of measurements on the perpendicular cross section of the moulded bar we were able to construct a map of the platelets alignment through the entire cross-section of the injection moulded sample and subsequently calculate an average orientation. The average 'shoulder width' at this local length scales is 13.7° and $\langle\cos^2(\delta\chi)\rangle = 0.94$. This value is close to 1, which is an indication of a very good alignment of the platelets in injection moulded samples, and it confirms the results of several authors [10,29,30]. The real orientation is probably even higher, as it would require deconvolution of the scattering signal with the X-ray line width. In any case, it may comfortably be assumed that there is a very high degree of platelets orientation in the mechanical modelling below. Any misalignment that might affect the calculated effective aspect ratio has the same influence on all moisture concentrations, and will not influence the conclusions.

4.3. Calculation of the modulus of the matrix phase

The moduli of the amorphous part of the matrix (consisting of amorphous PA6 and surfactant), which are used in the calculation of the nanocomposite matrix modulus, are shown in the fourth row in Table 2.

The modulus of dry PA6 is 3.10 GPa (measurement) and the amorphous modulus of dry PA6 is assumed to be 2.2 GPa (calculated from measurements [23]). With the Halpin–Tsai model a crystalline modulus of 5.25 GPa is calculated based on the crystalline volume fraction as shown in Table 2. This value for the crystalline modulus is similar to literature data, calculated from PA6 fibres [31]. It is assumed in the model that the α and γ-crystals have equal moduli, which is believed to be a reasonable assumption

Table 2
Results matrix modulus calculation with the Halpin–Tsai model

	Pure PA6	2.6%	4.7%	6.8%	8.3%	10.6%
Properties matrix (PA6 + surfactant)						
wt% silicate (TGA)	0	2.6	4.7	6.8	8.3	10.6
vol% surfactant in matrix	0	1.52	2.79	4.11	5.12	6.71
vol. fraction surf. in amorphous matrix	0	0.022	0.042	0.060	0.073	0.093
$E_{\text{amorphous matrix}}$, dry [GPa]	2.20	2.15	2.11	2.07	2.04	2.00
$E_{\text{amorphous matrix}}$, 3% water [GPa]	0.31	0.30	0.30	0.29	0.29	0.28
$E_{\text{amorphous matrix}}$, 6% water [GPa]	0.038	0.037	0.037	0.036	0.036	0.035
Matrix moduli (calculated)						
E_{matrix}, dry [GPa]	3.10	3.06	3.01	2.94	2.87	2.81
E_{matrix}, 3% water [GPa]	1.29	1.28	1.25	1.20	1.15	1.09
E_{matrix}, 6% water [GPa]	0.82	0.82	0.80	0.76	0.72	0.67

because the hydrogen bond density is very similar. The value of 5.25 GPa for the crystalline phase is assumed to be independent of moisture conditioning and is used in all further calculations.

The Halpin–Tsai model is also used to estimate the amorphous modulus in moisture conditioned samples. The measured values for moisture conditioned PA6 are 1.29 GPa for 3% water and 0.82 GPa for 6% water, and with the value of 5.25 GPa for the crystalline modulus this leads to the amorphous moduli shown in Table 2. For a moisture level of 3% the calculated amorphous modulus is 0.31 GPa and for a moisture level of 6% it is 0.038 GPa; this large drop in amorphous modulus is expected because at 3% water the amorphous part of the PA6 has crossed T_g, reaching the rubber plateau. In the fourth row the results for the dry amorphous modulus at the various filler levels are shown, in the fifth and sixth row the results for the moisture-conditioned amorphous moduli are shown. The decrease in the amorphous modulus with increasing silicate content is caused by the increasing amount of surfactant.

In the next step for each silicate concentration and moisture content a value for the nanocomposite matrix modulus was calculated using the Halpin–Tsai equation. The values for the modulus (5.25 GPa) and the aspect ratio ($w/t = 1000$) of the crystalline lamellae are chosen to be constant. For each sample the specific crystalline volume fraction (Table 1) and the amorphous matrix modulus (Table 2) were used. The resulting nanocomposite matrix modulus for each sample is shown in the last three rows of Table 2 and in Fig. 7.

The results of the calculated matrix moduli are independent on the average orientation or on the aspect ratio of the crystalline plates that is assumed. This is because the modulus of the moisture-conditioned amorphous phase is basically a fit-parameter to describe the measured modulus of the moisture-conditioned unfilled PA6 samples. Therefore, if the aspect ratio would be assumed to be smaller, the estimated modulus of the moisture conditioned amorphous matrix would be higher, and vice versa. The same applies for the orientation; if the platelets would not be considered completely random but partially aligned, the model would result in a lower amorphous matrix modulus. The calculated dependence of the matrix modulus on the silicate content is independent on the crystalline aspect ratio or orientation (within reasonable limits). It is important to realize that the Halpin–Tsai model that is used to calculate the matrix modulus is not intended to provide an accurate prediction of the aspect ratio of the crystalline lamellae or the moduli of the different phases. It is only used to calculate the influence of the modified silicate particles on the matrix modulus by introducing the effect of the surface modification and the small change in crystallinity.

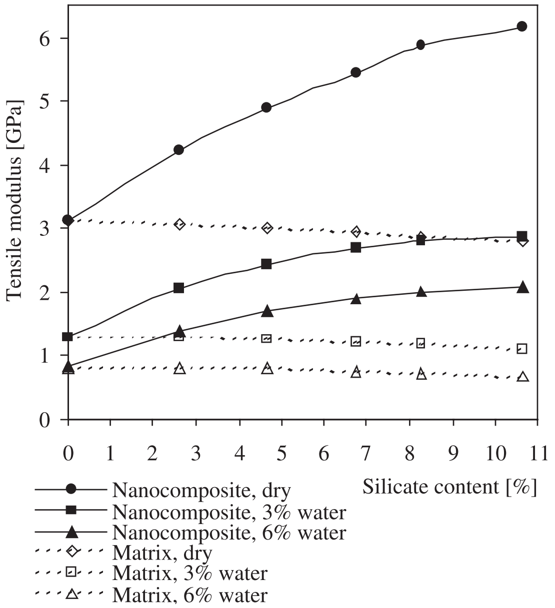

Fig. 7. Influence of silicate and moisture content on the tensile modulus.

4.4. Modulus of the nanocomposites and calculation of the aspect ratios

4.4.1. Modulus

The measured results for the tensile modulus of the nanocomposite samples at various moisture contents and silicate concentrations are shown in Fig. 7, along with the calculated matrix moduli that are used in the model. A reduction of the stiffness is clear for both the unfilled polymer (at 0% silicate) and the nanocomposites when water is absorbed during conditioning. The previously calculated matrix moduli (Table 2) were used in the Halpin–Tsai model to calculate the effective aspect ratios. These calculated aspect ratios are shown in the last three rows in Table 3 and Fig. 8.

The calculated effective aspect ratios are based on particles aligned with their long dimensions along the test axis, which is a reasonable assumption as was shown in Section 4.2. It can be seen in Fig. 8 that the effective aspect ratio decreases with increasing silicate content, which can be

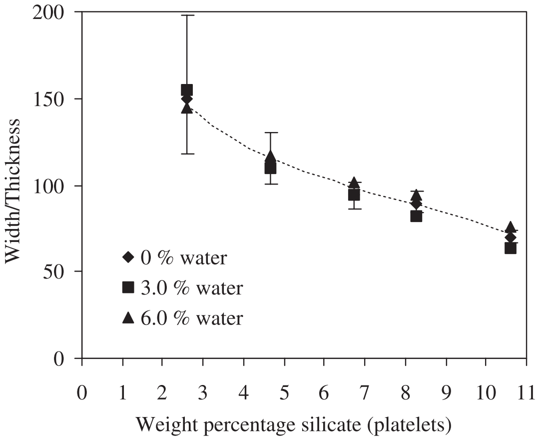

Fig. 8. Calculated aspect ratios versus silicate content.

Table 3
Nanocomposite moduli and calculated aspect ratios from Halpin–Tsai model

Nanocomposite moduli	Pure PA6	2.6%	4.7%	6.8%	8.3%	10.6%
Dry [GPa]	3.10	4.21	4.88	5.44	5.86	6.21
3% Water [GPa]	1.29	2.07	2.41	2.70	2.81	2.86
6% Water [GPa]	0.82	1.39	1.69	1.90	2.01	2.07

Effective aspect ratios	2.6%	4.7%	6.8%	8.3%	10.6%
Dry	152	114	95	89	70
3% Water	155	110	94	82	64
6% Water	145	117	102	94	75

explained by a less effective exfoliation at higher silicate loadings. The reduced exfoliation at higher silicate content has been shown previously by several authors [7,13,32]. It is also in agreement with calculations based on diffusion and melt-viscosity data, which will be published in separate papers [18,33].

The most important result from these aspect ratio calculations is the fact that the data for three different moisture contents overlap in Fig. 8. This shows that the modulus of a nanocomposite can be explained by the combination of a very stiff filler particle with a high aspect ratio and the normal matrix modulus, which in this case is varied by changing the moisture content. Apparently, the Halpin–Tsai composite theory can be used to describe the stiffness of nanocomposites for a wide variety of matrix moduli, both below and above T_g of the matrix polymer, with the same aspect ratio for all matrix moduli. The fact that the modulus of nanocomposites can be explained by the Halpin–Tsai theory independent on the modulus of the matrix proves that the reinforcing mechanism in nanocomposites is similar to traditional composites. No additional stiffening of the matrix due to confinement of the polymer has to be assumed to explain the modulus of nanocomposites.

To show the influence of errors in the modulus measurements, error bars are displayed for the dry series in Fig. 8 (for clarity the other series do not show the error bars). The error bars correspond to a constant error of ± 0.1 GPa in the modulus measurement. It can be seen that at low silicate concentrations a small error in the modulus measurement has large effects on the calculated aspect ratio; however, for higher concentrations the error is much smaller and the calculated aspect ratios are more reliable. It is clear that based on these calculations it has to be concluded that the effective reinforcing effect of the particles seems to decrease with increasing silicate loading. The effective aspect ratios from the model are realistic values: the aspect ratios are between 70 and 150, which is in the range of what was observed in the TEM picture shown in Fig. 9.

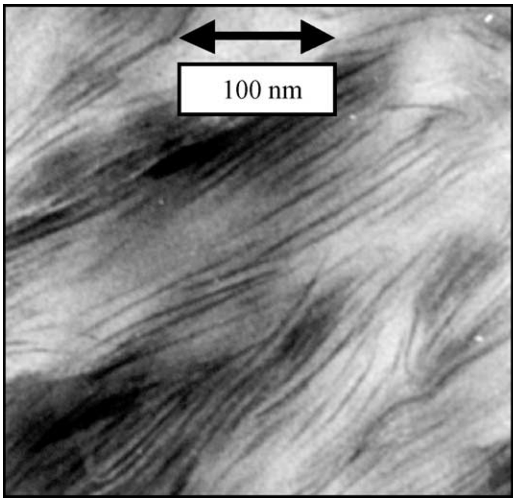

Fig. 9. 2.6% cloisite 30B (TEM).

With increasing concentration the exfoliation becomes less perfect, resulting in an effective aspect ratio that is half of the highest value. This means that when perfect exfoliation is assumed in the low concentrations, an average stack size of two platelets is present in the highest concentrations.

As a final point of discussion it is emphasized that the Halpin–Tsai model is a semi-empirical model. The aspect ratio's reported here are, therefore, effective values, incorporating effects of distribution, polydispersity and shape variability. It appears from this study that the Halpin–Tsai model is sufficiently accurate to describe the reinforcing power of nanoplatelets in a single parameter, the effective aspect ratio. Note that the effective aspect ratio is more than a fitting parameter since the nanocomposite stiffness at all the different moisture levels can be explained by the same effective aspect ratio (for each silicate content).

5. Conclusions

Because the modulus of the PA6 matrix can be adjusted by varying the amount of absorbed water, the nanocomposite series used in this study is very useful to investigate if the nanocomposite modulus can be described with a conventional composite theory such as the Halpin–Tsai theory.

The layered silicate used in this study induces a different crystalline phase in the polymer, and causes a small reduction of the crystallinity. WAXS measurements on the injection-moulded samples have shown that the PA6 crystals show a certain degree of alignment at the local level. However, when all different areas and both crystal phases are considered, the average alignment in the entire sample seems to be almost isotropic. Therefore, the Halpin–Tsai model with shape factors for platelet-shaped reinforcement and random alignment is used to estimate the modulus of the matrix in the nanocomposites as a function of crystallinity and surfactant content. The calculations show that with increasing silicate content the matrix modulus decreases slightly compared to the reference polymer, due to the reduced crystallinity and the dilution of the matrix by the surfactant.

The WAXS measurements trough the cross section revealed that the silicate layers are very well aligned in the flow direction in most of the sample volume. The calculated matrix modulus and the measured nanocomposite modulus for each sample is used in the Halpin–Tsai model for aligned platelets to calculate the effective aspect ratio of the silicate platelets for each concentration and moisture content. If the nanocomposite modulus is governed by the same mechanism as traditional composites, the effective aspect ratios that are calculated with the model should not depend on the matrix modulus. This is indeed found to be the case; all nanocomposites with different moisture content can be described with one aspect ratio for each silicate concentration. With increasing silicate concentration the calculated effective aspect ratio decreases, probably because of a reduced exfoliation of the silicate filler at higher loading. The effective aspect ratios derived from the model show a good similarity with the aspect ratios as they are observed in transmission electron microscopy, and the reduction of the effective aspect ratio can be explained by the appearance of small stacks of on average two platelets at the highest concentration. Therefore, it can be concluded that the high aspect ratio and high modulus of the platelets are the main reason for the strong increase of the modulus at a much lower filler content compared to micro-composites. The present results show that with the same microstructure (i.e. equal aspect ratio particles) the model is able to predict the measured modulus without requiring any major change of the matrix properties. The small change in modulus due to the different crystallinity and the addition of surfactant molecules was taken into account. In addition, a reduced mobility of the polymer phase would be unlikely to have much effect at temperatures below T_g, since the amorphous phase is rigid at those temperatures, but would have a larger influence above T_g. The Halpin–Tsai composite theory can be used to describe the modulus of nanocomposites both below and above T_g of the matrix polymer using the same aspect ratios. The results described here for different matrix moduli support the theories of Van Es and Fornes [9,10]. The shape and modulus of the reinforcing particles is sufficient to account for the observed moduli, without a special influence of their exceptionally small size or surface area, and without significantly influencing the modulus of the matrix. Changes on the molecular level due to the presence of the silicate layers apparently only have a small influence on the modulus. The reduced efficiency of reinforcement of the silicate sheets at increasing filler levels can be partially explained by the reduction of the matrix modulus due to the presence of surfactant and reduced crystallinity, and partially by the occurrence of small stacks of platelets.

Acknowledgements

The work of D.P.N. Vlasveld and S.J. Picken forms part of the research program of the Dutch Polymer Institute (DPI). The authors would like to thank Reinoud Gaymans of the University of Twente for the use of their injection molding equipment and Douwe Homminga of the KU Leuven for the TEM image of the nanocomposite.

References

[1] Kojima Y, Usuki A, Kawasumi M, Okada A, Fukushima Y, Kurauchi T, et al. J Mater Res 1993;8(5):1185–9.
[2] Usuki A, Kawasumi M, Kojima Y, Okada A, Kurauchi T, Kamigaito O. J Mater Res 1993;8(5):1174–8.
[3] Usuki A, Kojima Y, Kawasumi M, Okada A, Fukushima Y, Kurauchi T, et al. J Mater Res 1993;8(5):1179–84.
[4] Vaia RA, Ishii H, Giannelis EP. Chem Mater 1993;5(12):1694–6.
[5] Vaia RA, Giannelis EP. Macromolecules 1997;30(25):8000–9.
[6] Kawasumi M, Hasegawa N, Kato M, Usuki A, Okada A. Macromolecules 1997;30(20):6333–8.
[7] Akkapeddi MK. Polym Compos 2000;21(4):576–85.
[8] Cho JW, Paul DR. Polymer 2001;42(3):1083–94.
[9] Es MAv, Xiqiao F, Turnhout Jv, Giessen Evd. Specialty polymer additives. Oxford: Blackwell Science; 2001 [chapter 21].
[10] Fornes TD, Paul DR. Polymer 2003;44(17):4993–5013.
[11] Yoon PJ, Fornes TD, Paul DR. Polymer 2002;43(25):6727–41.
[12] Okada A, Usuki A. Mater Sci Eng C 1995;3(2):109–15.
[13] Es MAv. Thesis: polymer clay nanocomposites. The importance of particle dimensions. Delft: Delft University of Technology; 2001.
[14] Shelley JS, Mather PT, DeVries KL. Polymer 2001;42(13):5849–58.
[15] Giannelis EP. Adv Mater 1996;8(1):29.
[16] Usuki A, Koiwai A, Kojima Y, Kawasumi M, Okada A, Kurauchi T, et al. J Appl Polym Sci 1995;55(1):119–23.
[17] Hasegawa N, Okamoto H, Kato M, Usuki A, Sato N. Polymer 2003;44(10):2933–7.
[18] Vlasveld DPN, Bersee HEN, Picken SJ. Polymer, submitted for publication.
[19] Kojima Y, Usuki A, Kawasumi M, Okada A, Kurauchi T, Kamigaito O. J Appl Polym Sci 1993;49(7):1259–64.
[20] Kohan MI. Nylon plastics handbook. Munich: Carl Hanser Verlag; 1995.
[21] Halpin JC, Kardos JL. Polym Eng Sci 1976;16(5):344–52.
[22] Halpin JC. J Compos Mater 1969;3:732–4.
[23] Bureau MN, Denault J, Cole KC, Enright GD. Polym Eng Sci 2002;42(9):1897–906.
[24] Hsia KJ, Xin YB, Lin L. J Mater Sci 1994;29(6):1601–11.
[25] Shell HR, Ivey KH. Fluorine micas: Bureau of mines, US Department of the interior; 1969.
[26] Akzo Nobel Surface Chemistry website; 2004.
[27] Fornes TD, Paul DR. Polymer 2003;44(14):3945–61.
[28] Rothon R. Particulate-filled polymer composites. London: Longman; 1995.

[29] Kojima Y, Usuki A, Kawasumi M, Okada A, Kurauchi T, Kamigaito O, et al. J Polym Sci, Part B: Polym Phys 1995;33(7): 1039–45.

[30] Varlot K, Reynaud E, Kloppfer MH, Vigier G, Varlet J. J Polym Sci, Part B: Polym Phys 2001;39(12):1360–70.

[31] Murthy NS, Grubb DT. J Polym Sci, Part B: Polym Phys 2002;40(8): 691–705.

[32] Liu L, Qi Z, Zhu X. J Appl Polym Sci 1999;71:1133–8.

[33] Vlasveld DPN, De Jong M,, Bersee HEN, Gotsis AD, Picken SJ. Polymer, submitted for publication.